Preliminary application of 3.0T magnetic resonance chemical exchange saturation transfer imaging in brain metastasis of lung cancer

Yonggui Yang
The Second Affiliated Hospital of Xiamen Medical College https://orcid.org/0000-0001-5122-159X
Xiaobo QU
Department of Electronic Science,Fujian Provincial Key Laboratory of Plasma and Magnetic Resonance,Xiamen University
Yihui HUANG
Department of Electronic Science,Fujian Provincial Key Laboratory of Plasma and Magnetic Resonance,Xiamen University
Gang GUO
The Second Affiliated Hospital of Xiamen Medical College
Shaoyin DUAN (xmdsy@xmu.edu.cn)

Research article

Keywords: Magnetic Resonance Imaging(MRI), Chemical Exchange Saturation Transfer(CEST), Brain Metastases Of Lung Cancer, Magnetization Transfer Ratio(MTR)

Posted Date: August 30th, 2019

DOI: https://doi.org/10.21203/rs.2.11304/v1

Version of Record: A version of this preprint was published on January 13th, 2020. See the published version at https://doi.org/10.1186/s12880-019-0400-y.

Abstract

Background: Brain-metastasis of lung-cancer is very common and serious, and it is also one of the common causes of treatment failure. To investigate the clinical application of CEST technology in the diagnosis and prognosis evaluation of brain metastasis of lung cancer.

Methods: 26 cases of lung cancer brain metastases, 15 cases of gliomas and 20 cases of normal controls were collected. MTR(3.5ppm) image obtained by GRE-EPI-CEST sequence using ASSET technique and APT software was observed. MTR-values(3.5ppm) were measured in the lesion-parenchymal, edema and non-focus areas, and the MTR image was compared with the conventional MRI. Statistical-Tests were ANOVA and t-test.

Results:In the metastatic-tumor-group, the lesion-parenchymal, edema and non-focus areas were red-yellow, yellow-green, and green-blue, and the MTR-values were 3.29 ±1.14%,1.28 ±0.36%,1.26 ±0.31%. In glioma-group, the lesion-parenchymal, edema and non-focus areas were red, red-yellow, and the MTR-values of green-blue were 6.29 ±1.58%, 2.87 ±0.65%, 1.03 ±0.30%. The MTR-values of the corresponding areas in the normal-group were 1.07 ±0.22%,1.04 ±0.23%,1.06 ±0.24%. Traditional MR-images are in black-white contrast and no metabolic information is displayed. The MTR-values of three regions in metastatic-tumor-group and normal-group and glioma-group were significantly different, and the parenchymal area and edema area in metastatic-tumor-group were significantly different. There were significant differences in MTR-values between the non-lesion and edema areas, but there was no significant difference between the MTR-values in the edema area and the non-focus area. In glioma-group, there were significant differences in MTR-values between the parenchymal and edema areas and the non-focus areas, and the MTR-values between the edema and non-focus areas were significantly different.

Conclusions: CEST can obtained the pseudo-color-images, which can reflect protein metabolism. In metastatic-tumor-group, the parenchymal area was red-yellow, green-blue, and the MTR-value was lower than that of glioma group, higher than that of normal-group. Observed the MTR-image color and MTR-value, the early diagnosis of brain metastases and the prognosis evaluation can be achieved on the molecular-imaging level. Trial registration: Grant No. 3502Z20144052.The experiments in the article did not involve the results of health care interventions for human participants.

Background

Metabolic balance and acid-base balance are important components to maintain the homeostasis of the body [1]. So, in the early stages of the disease, the changes in intracellular and extracellular metabolites and pH values have received much attention. As an important branch of magnetic resonance imaging (MRI), chemical exchange saturation

transfer (CEST) has the advantages of non-radiative, non-invasive, selective T_1 and T_2 contrast and metabolic imaging [2,3], which extends MRI from traditional anatomical imaging to living metabolic imaging, pH imaging and other organisms. Moreover, it expands the new field of molecular imaging MRI, providing a new detection method for the diagnosis, treatment and even prevention of clinical diseases.

Brain metastasis of lung cancer is very common and serious, and is also one of the common causes of treatment failure[4,5]. How to monitor the changes of metabolites in the course of brain metastases is a problem, and CEST provides a new method to solve it. This article aims to investigate the clinical application of 3.0T MRI CEST technology in the diagnosis and prognosis evaluation of brain metastasis of lung cancer.

Methods

General Information

From January to July 2018, 26 cases of lung cancer brain metastases(17 males and 9 females, their ages were 48-73 years old, and average was 51.36 years old), 15 cases of gliomas (10 males and 5 females, their age was 38-48 years old, and average was 43.20 years) and 20 cases of normal controls (14 males and 6 females, their ages were 24-29 years old, and average was 25.87 years) were collected. The primary tumor of 26 cases of brain metastases was lung cancer, including 8 cases of adenocarcinoma, 4 cases of small cell lung cancer, 11 cases of squamous cell carcinoma, and 3 cases of large cell lung cancer.

The research project was reviewed and approved by the Medical Ethics Committee of The Second Affiliated Hospital of Xiamen Medical College (the Medical Ethics Committee of Xiamen No.2 Hospital,Approval No: 2014004). All subjects were informed of the examination and signed informed consent before the examination. And it had informed consent written was obtained from all participants .

Imaging method

Routine MRI examination (T1WI, T2WI, T2 FLAIR), enhanced examination (T1WI+C), diffusion weighted imaging (DWI), Susceptibility Weighted Imaging (SWI), Arterial Spin Labeling (ASL), and CEST were acquired by GE Discovery Silent (750W) 3.0T MRI.

The CEST imaging parameters are as follows:

OAx CEST imaging: Gradient Recalled Echo Echo planar Imaging (GRE EPI) CEST sequence using Array Spatial Sensitivity Encoding Technique(ASSET), NEX=1, TR=2000ms, TE=Minimum, Number of Shots=1, Flip Angle=20°, FOV=24cm×24cm, Matrix=128×128, Number of Frequency=128, Number of Phase=128, Frequency Direction=R/L, Slice Thickness=4 mm, Spacing=0 mm. Number of Slices = 1 Slice, Acquisition Time: 1 minute 44 seconds.

Inclusion and exclusion criteria

Inclusion criteria:

All patients were confirmed by clinical and pathological findings, and MRI data and other related data were complete.

Two high-grade imaging doctors participated the inclusion procedure, whose experience in imaging diagnosis for more than 10 years and attending physician has been more than 3 years old. They combined the above data with MRI, including metastatic tumors or intracranial primary tumors, lesion location, number, size, morphology, imaging diagnosis and differential analysis of tumor signal manifestations, lesion enhancement, and edema around the tumor. At the same time, tumor blood supply and bleeding were observed by SWI images. The two doctors read the films independently, and the consistent summary opinions were confirmed as valid.

Patients who were consistently confirmed as normal were included in the normal group, lung cancer brain metastases were included in the metastatic tumor group, and high-grade gliomas were included in the glioma group.

Exclusion criteria:

Image data cannot meet the diagnostic requirements.

The lesion is less than 1 cm, or the SWI is characterized by intratumoral bleeding.

Data Processing and Analysis

The post-processing of CEST was performed using the ADW4.6 workstation function tool 2.0 Research version APT software. The observed 3.5ppm magnetization transfer rate (MTR) map was used to compute the MTR value of lesion parenchymal area, edema area and non-focal area , measured in %, compared to plain scan, enhancement, DWI, SWI, ASL images of a 3.0T MRI instrument.

When drawing the region of interest, we refer to the signal dominated by enhanced and DWI images, to avoid cysts and necrotic areas. The lesion parenchymal area was selected to be the most prominent area in the lesion or the lower ADC value of the DWI. In combination with T_2 FLAIR and enhancement, the edema area was selected in the edema area within 2 cm of the tumor. The non-lesional area was selected in the normal white matter area on the contralateral side. All areas are selected to avoid blood supply vascular areas and cerebrospinal fluid areas as much as possible.

The measured data was expressed by (mean ± standard deviation) and statistical analysis was performed using SPSS 23.0 from IBM. The MTR values of the focal parenchymal area, the edema area, and the non-lesional area,which of the normal group, the metastatic tumor group, and the glioma group, and the corresponding areas between the groups were first analyzed by one-way ANOVA, with test standard $\alpha=0.05$. When the one-way ANOVA analysis of variance was $P<0.05$, the independent sample t-test with the mean number of samples was compared. With test standard $\alpha=0.05$, $P<0.05$ was considered statistically significant.

Results

GRE EPI CEST sequence using ASSET technology, NEX=1, TR=2000ms, TE=Minimum, Number of Shots=1, Flip Angle=20^o, FOV=24cm×24cm, Matrix=128×128, Number of

Frequency=128, Number of Phase=128, Frequency Direction=R/L, Slice Thickness=4 mm, Spacing=0 mm. On the MTR map, the focal parenchymal areas, the edema areas, and the non-lesional areas of the metastatic tumor group were reddish yellow, yellowish green, and greenish blue, respectively, and the MTR values were 3.29±1.14%, 1.28±0.36%, and 1.26±0.31%, respectively. These areas of glioma group was red, reddish yellow, and greenish blue, and the boundary between the parenchyma and the edema was unclear. The corresponding MTR values were 6.29±1.58%, 2.87±0.65%, and 1.03±0.30%. The same areas of the normal group were greenish blue, and the MTR values were 1.07±0.22%, 1.04±0.23%, and 1.06±0.24%. Traditional MRI images are in black and white contrast with no metabolic information(Figures 1, 2, 3, 4 and Table 1).

The results of one-way ANOVA analysis of variance show that, the MTR values in the focal parenchymal areas, the edema areas, and the non-lesional areas of the normal group were F=0.074, P=0.929>0.05, no statistical difference. And the MTR values in the focal parenchymal areas, the edema areas, and the non-lesional areas of different groups and between different groups were P <0.05, both have statistical differences.

When it comes to metastatic tumor group and normal group (t=-8.550, -2.994, -2.403, P=0.000, 0.024, 0.021), glioma group (t=-6.437, -8.399, 2.382, P=0.000, 0.000, 0.024), the corresponding MTR values of the corresponding three regions which in the focal parenchymal areas, the edema areas, and the non-lesional areas were statistically different (P<0.05), as shown in Table 2. The MTR values in the focal parenchymal areasof the metastatic tumor group were compared withwhich in the edema areas (t=7.207, P=0.000) and in the non-lesional areas(t=8.762, P=0.000), were all statistically different (P<0.05). The MTR values in the edema areas, and the non-lesional areas were compared, t=0.188, P=0.852, and there was no statistical difference (P>0.05). The MTR values in the focal parenchymal areas of the glioma group were compared with which in the edema areas (t=7.748, P=0.000) and in the non-lesional areas(t=12.672, P=0.000), and all were statistically different (P<0.05). The MTR values in the edema areas, and the non-lesional areaswere compared, t=9.926, P=0.000, and there was a statistical difference (P<0.05), as shown in Table 3.

Discussion

Combination of multiple MRI techniques for brain metastases

Traditional magnetic resonance diagnosis of brain metastases is performed by routine MRI and enhanced examination, and the signals of brain metastases and edema around the tumor are observed. That is, the MRI shows that the brain metastases are slightly low or low signal intensity on T_1 WI, high signal intensity on T_2WI, equal or slightly low signal intensity on T_1 WI and high signal intensity on T_2WI in the edema area around the tumor. The reason is tumor cells have a relatively high water content compared with normal white matter. By MR-enhanced scans, brain metastases had characteristic of uniform enhancement, uneven enhancement, nodular or annular enhancement, and more clearly showed partially hidden lesions. The edemas around the tumor are not enhanced. When brain metastases intratumoral hemorrhage occur, complicated by hypertension, some lesions showed high or slightly high signal on T_1WI.

The DWI and its ADC signals were used to observe the degree of edema of lung cancer and its surrounding edema. when high DWI signal and decreased ADC value appear, it reflected the changes of microscopic structure of brain metastasis, and showed certain characteristics to the surrounding area of the tumor. So it can effectively improve the accuracy of diagnosis and differential diagnosis of lung cancer brain metastases. This is well validated in this set of data[6].

SWI showed tumor and peripheral blood supply, intratumoral hemorrhage, non-invasive detection of differences in magnetic sensitivity between tissues, reflecting blood oxygen levels in tissues. In this group of data, 26 cases of brain metastases and 15 cases of gliomas, SWI images showed a low intra-tumor signal and connected with the blood supply artery. Cases of brain metastases and gliomas with intratumoral hemorrhage were excluded by SWI images to avoid affecting CEST MTR results[7,8].

Using ASL with PLD=2.0, it is possible to determine the changes in blood-brain barrier permeability and the loss of cerebral blood flow regulation during the evolution of brain

metastases and gliomas[9].

The role of 3.0T MR CEST

In the experiment, T1WI, T2WI, T2 FLAIR, T1WI+C, DWI, SWI, ASL of 3.0T MRI were used to verify and observe the metastatic tumor group, glioma group and normal group. Using the GRE EPI CEST sequence of ASSET technology, the 3.5ppm (MTR) map were obtained by APT software with the quantitative analysis of the corresponding region. Then, the CEST technique and clinical application value of 3.0T magnetic resonance lung cancer brain metastasis were discussed. The aim is to develop a non-invasive and accurate molecular imaging MRI research program based on CEST for lung cancer brain metastases. The results showed the characteristics of CEST signal in lung cancer brain metastasis. The focal parenchymal areas and edema areas of the metastatic tumor group were reddish yellow and greenish blue. The MTR value was lower than that of the glioma group, which was higher than the normal group. But the non-lesional areas of the metastatic tumor group were greenish blue. The MTR value is higher than glioma group, normal group. The MTR values of the edema and non-lesional areas are similar. In addition, these value were higher than those in the normal group, which were mainly in the substantial region (Figures 1, 2, 3, and 4) [10,11].

This is related to the mechanism of brain metastases derived from hematogenous metastasis. The tumor cells circulate in various parts of the body with blood, including the parts of the brain where no metastatic lesions have been found. Thus the MTR value of the metastatic tumor lesions is significantly increased. And the MTR value in the edema areas, and the non-lesional areas are increase.

When the brain metastases are accompanied by hemorrhage, the high MTR value of the parenchymal area, and the signal in the focal parenchymal areasis uneven. This is related to the oxygenated hemoglobin content, the deoxyhemoglobin content, and the necrosis of the tumor parenchyma in different periods after hemorrhage. Conventional sequences combined with SWI and ASL can verify it. when SWI showed old bleeding with a significantly low signal, the MTR value reach more than 80% increase. Although the

parenchymal areas are all increased, the differences between individuals and regions are large, which may be related to the coexistence of new and old hemorrhage in the metastatic tumor and necrosis in the tumor [7,8]. CEST can detect blood products (deoxyhemoglobin, methemoglobin, ferritin, and hemosiderin) that cause hemorrhage and a significant increase in MTR. It may also be related to changes in tissue pH during the evolution of brain metastatic tumors, which requires further data validation. In order to avoid the interference of bleeding, the cases of intratumoral bleeding were not included in the data of this group.

PTBE will make the tumor occupying effect more obvious, further increase intracranial pressure and worsen clinical symptoms. In MRI, the signal of edema around the tumor of brain metastases is varies. This is not only related to the macroscopic factors such as the specificity of the nervous system, the location of the brain metastases and the degree of malignancy, but also VEGF and its receptors, AQP-4, MMP-9, IL-6, HIF-1a and other molecular organisms factors [5,12]. In this data, VEGF and AQP-4 results showed high levels of high expression. Especially in cases with peri-tumoral edema, AQP-4 was highly expressed in brain tissue surrounding brain metastatic tumors, not within metastatic tumors. This explains why the MTR value of CEST in brain metastases is increased, and the MTR value in the edema and non-focal areas is more pronounced in cases with bleeding, which may also promote angiogenesis with VEGF. It is related to factors such as the destruction of the blood-brain barrier. The edema around the tumor is related to the malignant degree of the tumor. The edema around the tumor caused by the malignant tumor destroying the blood-brain barrier is mainly angiogenic. And the edema mainly invades the white matter of the brain, and the liquid with a small amount of protein is damaged due to the damage of the blood-brain barrier, and accumulate around the tumor. The degree and extent of edema around the tumor are related to the structure and characteristics of the brain tissue itself. For example, edema in the cortex, basal ganglia, and thalamus is not easy to occur. The edema in the white matter area is more obvious, but not in the brain stem. In this group of data, this was also verified that 8 cases of edema-free brain metastases occurred in the basal ganglia and thalamus.

The MTR values in the focal parenchymal areasof the glioma group were higher than that of the metastatic tumor group. In addition, the lesion parenchyma and edema area were red, reddish yellow, and their boundary was unclear. The non-lesional area was greenish blue, and not different from the normal group with no increment.

The MTR values in the focal parenchymal areas of the metastatic tumor group were higher than those in the edema area and the non-focal area. The MTR values in the edema areas, and the non-lesional areas were similar, which were slightly higher than normal.

In this paper, CEST mainly reflects not only the metabolism of free protein and peptide molecules, but also the tumor activity and its progress from the molecular level[13-19]. The MTR values in the edema areas of the glioma group are increased, which is consistent with the tumor surrounding the brain and the surrounding edema of the tumor. However, brain metastases do not invade, but compression, the secondary edema of brain metastases occurs, which is differentiated from the original tumors in the brain. CEST has certain advantages in sensitivity and accurate display of anatomical structure. It can visually observe the abundant free protein or polypeptide molecules in brain metastases. Moreover, it is important for its treatment and prognosis that early diagnosis and comprehensive evaluation of the scope of brain metastases and its surrounding anatomical structure [13,19-22].

Case selection principles and limitations

As a material basis of life, proteins are closely related to various forms of life activities. Protein accounts for 16% to 20% of body weight, and its amide proton content is high[13,19-22]. The lung cancer brain metastasis and high-grade gliomas in this study have abnormal metabolism of intracellular proteins and peptides in their own disease course. This is the material basis of CEST effect in APT imaging, which is used to distinguish between parenchymal and necrotic areas, surrounding edema area, etc.

Brain metastases account for 10% to 15% of intracranial tumors, and lung cancer brain metastases account for 30%-40%[4]. This is also the reason why the experimental data

cases are included in the above diseases.

The purpose of this experiment was to verify the CEST imaging effect. All of the selected brain metastases were lung cancer. Because the brain metastases of different types of lung cancer, brain metastases of different degrees, edema and edema size were not analyzed. So this brings the limitations of analysis, and will refine the research in the future work.

At present, there are still some cases of low signal-to-noise ratio and unsatisfactory contrast in CEST image quality. Combined with conventional sequence and enhanced examination, a certain degree of registration and correction are profitable to display and distinguish lesions, and analyze brain metastases. The regional signal and its MTR value can distinguish lesion parenchyma, necrosis and peripheral edema (Figures 2, 3, 4).

The experimental group will further collect data, expand the range of disease types, randomly select data, and analyze specificity and sensitivity. At the same time ,we will in-depth study the fast APT imaging sequences, and strive to use the fast imaging sequence software package. So as to reduce the series of interference signals caused by the EPI sequence, realize the intelligent CEST-APT imaging, and provide intelligent and accurate molecular imaging diagnosis information for the research of brain diseases.

Conclusions

The CEST sequence and APT software using ASSET and GRE-EPI techniques obtain pseudo-color images and reflect protein metabolism. The metastatic area and edema area of the metastatic tumor group were reddish yellow and greenish blue. The MTR value was lower than that of the glioma group, which was higher than that of the normal group. The non-focal area was greenish blue, and the MTR value was higher than that of the glioma group and the normal group.

Combined with the sequence of sweep, enhancement, DWI/DKI, SWI, ASL/PWI and MRS, the MTR image color resolution and MTR value of CEST 3.5ppm acyl protons can be used to observe the distribution and metabolic changes of brain metastases and realize

early diagnosis of brain metastases and assessment of the outcome of molecular imaging of lesions.

Of course, the clinical application of CEST technology is still in the research stage, and further optimization is needed. It is believed that with the deepening of research, its clinical application value will become more and more extensive.

Abbreviations

T: Tesla; MRI: Magnetic Resonance Imaging; CEST: Chemical Exchange Saturation Transfer; MTR: Magnetization Transfer Ratio; ppm: parts per million; SE: spin echo; FSE: fast spin-echo; APT: amide proton transfer; RF: radio frequency; T1WI: T1 Weighted Imaging; T2WI: T2 Weighted Imaging; T2 FLAIR:T2 FLuid Attenuated Inversion Recovery; T1WI+C:enhanced examination (Contrast) of T1 Weighted Imaging; DWI: Diffusion Weighted Imaging; SWI: Susceptibility Weighted Imaging; ASL: Arterial Spin Labeling; GRE EPI: Gradient Recalled Echo Echo planar Imaging; ASSET: Array Spatial Sensitivity Encoding Technique; OAx: Oblique axis; TR: repetition time; TE: echo time; FOV: field of view; SNR: signal

to noise ratio; ROI: region of interest; VEGF: vascular endothelial growth factor; AQP: aquaporin; MMP: matrix metalloprotein-ase; IL: interleukin; HIF-1a: hypoxia inducible factor-1a;

Declarations

Ethics approval and consent to participate

The research project was reviewed and approved by the Medical Ethics Committee of The Second Affiliated Hospital of Xiamen Medical College (the Medical Ethics Committee of Xiamen No.2 Hospital,Approval No: 2014004). All subjects were informed of the examination and signed informed consent before the examination. And it had informed consent written was obtained from all participants .

Consent for publication

All presentations of case reports had consent for publication.

Availability of data and material

All data generated or analysed during this study are included in this published article.

Competing interests

The authors declare that they have no competing interests.

Funding

This work was supported by

1.Planned Project Grant (Grant No. 3502Z20144052) from the Science and Technology Bureau of Xiamen.

2.the Natural Science Foundation of Fujian Province of China under grant 2018J06018.

3. the Fundamental Research Funds for the Central Universities under grant 20720180056.

In the Funding section, the role of the funding body (Grant No. 3502Z20144052) in the design of the study and collection, analysis, and interpretation of data and in writing the manuscript. And the role of the funding body (Grant No. 2018J06018 and 20720180056) in the design of the interpretation of data and in writing the manuscript.

Authors' contributions

YY designed the entire experimental protocol. As a mentor, SD and GG guided the experimental process. Data collection and data analysis were performed by YY, XQ, YH, GG and SD. XQ is a member of the research team and sends his students to collect analytical data.All authors have been involved in drafting and revising the manuscript and approved the final version to be published. All authors read and approved the final manuscript.

Acknowledgements

The authors would like to thank all authors in this work.

Authors' information (optional)

Author Names and Degrees:

Yong-gui YANG1, MM.

Xiaobo QU2, PhD.

Yihui HUANG2.

Gang GUO 1*, MD.

Shaoyin DUAN 3*, PhD. MD.

Author Affiliations:

1.Dept. of Radiology Imaging，The Second Affiliated Hospital of Xiamen Medical College，Xiamen 361021;

2.Department of Electronic Science, Fujian Provincial Key Laboratory of Plasma and Magnetic Resonance, Xiamen University, Xiamen, Fujian Province, China;

3.Dept. of Radiology，Zhongshan Hospital Xiamen University, Xiamen, China;

Correspondence to:

Common Corresponding Author

Dr. Gang GUO, M.D.

Dept. of Radiology Imaging，The Second Affiliated Hospital of Xiamen Medical College

Xiamen, Fujian Province, China

Email: guogangxm@163.com

Dr. Shaoyin DUAN, PhD. MD.

Dept. of Radiology，Zhongshan Hospital Xiamen University, Xiamen, Fujian Province, China

Email: xmdsy@xmu.edu.cn

References

1. Sun P Z, Sorensen AG. Imaging pH using the chemical exchange saturation transfer (CEST)MRI: Correctionof concomitant RF irradiation effects to quantify CEST MRI for chemical exchange rate and pH [J].MagnResonMed, 2008,60(2):390–397.
2. Ward K M, Aletras A H, Balaban R S. A new class of contrast agents for MRI based on proton chemical exchange dependent saturation transfer (CEST) [J]. J Magn Reson, 2000, 143(1): 79-87.
3. Yang YG, Shen ZW, Wu RH,et al．Research of chemical exchange saturation transfer in brain[J].Chin J Magn Reson Imaging,2016, 7(4): 81–84.
4. MA Qian, MIAO Hong, ZHANG Shuai,et al.MR Findings of Brain Metastases from Different Primary Tumors[J].Chinese Journal of CT and MRI.2018,16(1):30-32.
5. GAO J,LIU YH, YAN L,et al.Research progress on peritumoral edema-related molecular biology factors of the metastasis tumor of brain[J].Chin J Clin Oncol,2014,41(8):534-537.
6. Wang E, Wu Y, Cheung JS, et al. pH imaging reveals worsened tissue acidification in diffusion kurtosis lesion than the kurtosis/diffusion lesion mismatch in an animal model of acute stroke. J Cereb Blood Flow Metab. 2017;37(10):3325-3333.
7. Liang S, Zhang FX.The value of SWI in diagnosis of brain metastases with lung cancer[J].Journal of Practical Medical Imaging,2017,18(1):7-9.

8. Li L, Liu SM, Li GQ, et al. Susceptibility-weighted Imaging in Thrombolytic Therapy of Acute Ischemic Stroke. Chinese Medical Journal.2017;130.
9. Mirasol RV, Bokkers RPH, Hernandez DA, et al. Assessing Reperfusion With Whole-Brain Arterial Spin Labeling. Stroke. 2014;45:456-461.
10. YANG YG, GUO G.The application of different NEX amide proton transferimaging in brain tumors on 1.5 T MRI scanner[J]. Chin J Magn Reson Imaging, 2017, 8(12):923-928.
11. YANG YG, CHEN Z, CAI CB,GUO G.Factors Affecting Chemical Exchange Saturation Transfer Imaging on 1.5 T Clinical MRI Scanners[J]. Chinese J Magn Reson, 2017, 34(3):275-282.
12. DONG P, WANG B, SUN XH,et al.Factors of the edema size of intracranial metastases from lung cancer[J].Chin J Med Imaging Technol.2006,22(1):57-60.
13. Zhou J, et al. Quantitative description of proton exchange processes between water and endogenous and exogenous agents for WEX, CEST and APT experiments. Magn Reson Med, 2004, 51(5):945-952.
14. Van Zijl P CM, Yadav NN. Chemical exchange saturation transfer (CEST): What is in a name and what isn't? [J]. Magn Reson Med, 2011, 65(4): 927-948.
15. Zhou J, Lal B, Wilson DA,et al Amide proton transfer (APT) contrast for imaging of brain tumors [J]. Magn Reson Med, 2003, 50(6): 1120-1126.
16. Mcconnell H. M. Reaction rates by nuclear magnetic resonance [J]. J Chem Phys, 1958, 28(3): 430.
17. Mori S, Eleff SM, Pilatus U,et al Proton NMR spectroscopy of solvent-saturable resonances: A new approach to study pH effects in Situ [J]. Magn Reson Med, 1998, 40(1): 36-42.
18. Sun PZ, Longo DL, Hu W, et al.Quantification of iopamidol multi-site chemical exchange properties forratiometric chemicalexchange saturation transfer (CEST)imaging of pH. Physics in Medicine and Biology, 2014, 59(16): 4493-4504.

19. Sun PZ, Wang Y, Dai Z, et al. Quantitativechemical exchange saturation transfer(qCEST) MRI--RF spillover effect-correctedomega plot forsimultaneous determination of labile proton fraction ratio and exchange rate.Contrast Media & MolecularImaging, 2014,9(4): 268-275.
20. Sun P Z, Wang E, Cheung J S,et al□Simulation and optimization of pulsed radio frequency (RF)irradiation scheme for chemical exchange saturation transfer(CEST) MRI – demonstration of pH-weighted pulsed-amide proton CEST MRI in an animal model of acute cerebral ischemia[J].MagnResonMed,2011,66(4):1042–1048.
21. Sun PZ, Longo DL, Hu W, et al.Quantification of iopamidol multi-site chemical exchange properties forratiometric chemicalexchange saturation transfer (CEST)imaging of pH. Physics in Medicine and Biology, 2014, 59(16): 4493-4504.
22. Sun P Z, Wang E, Cheung J S. Imaging acute ischemic tissue acidosis with pH-sensitive endogenous amide proton transfer (APT) MRI-Correction of tissue relaxation and concomitant RF irradiation effects toward mapping quantitative cerebral tissue pH [J]. Neuroimage, 2012, 60(1): 1-6.

Tables

Table 1: One-way ANOVA variance test for MTR values in corresponding groups

Groups	Number of cases	the lesion parenchymal areas	the edema areas	the non focal areas		
		MTR's Mean ± standard deviation（%）			F value	P value
A	20	1.07±0.22	1.04±0.23	1.06±0.24	0.074	0.929
B	26	3.29±1.14	1.28±0.36	1.26±0.31	75.219	0.000
C	15	6.29±1.58	2.87±0.65	1.03±0.30	99.167	0.000
F value		98.741	87.420	4.160		
P value		0.000	0.000	0.002		

Note: $P < 0.05$, there is a statistical difference.

A: normal group; B: metastatic tumor group; C: glioma group;

Table 2: Independent sample t-test of MTR values in corresponding regions between groups

Compared	the lesion parenchymal areas				the edema areas				the non focal areas			
	Levene's Test		t test		Levene's Test		t test		Levene's Test		t test	
	F value	P value	t value	P value	F value	P value	t value	P value	F value	P value	t value	P value
normal group & metastatic tumor group	14.315	0.000	-8.550	0.000	0.597	0.445	-2.394	0.024	0.743	0.394	-2.403	0.021
normal group & glioma group	21.706	0.000	-14.642	0.000	6.538	0.015	-11.651	0.000	1.209	0.279	0.405	0.689
metastatic tumor group & glioma group	1.807	0.187	-6.437	0.000	2.959	0.095	-8.399	0.000	0.051	0.823	2.382	0.024

Note: Levene's Test, P<0.05, homogeneity of variance; independent sample t-test, P=<0.05, statistically significant;

Table 3: Independent sample t-test of MTR values between corresponding groups in each group

Compared	metastatic tumor group				glioma group			
	Levene's Test		t test		Levene's Test		t test	
	F value	P value	t value	P value	F value	P value	t value	P value
lesion parenchymal areas& edema areas	10.107	0.003	7.207	0.000	7.252	0.012	7.748	0.000
lesion parenchymal areas& non focal areas	15.738	0.000	8.762	0.000	14.365	0.001	12.672	0.000
the edema areas& non focal areas	0.066	0.798	0.188	0.852	3.153	0.087	9.926	0.000

Note: Levene's Test, P<0.05, homogeneity of variance; independent sample t-test, P=<0.05, statistically significant;

Figures

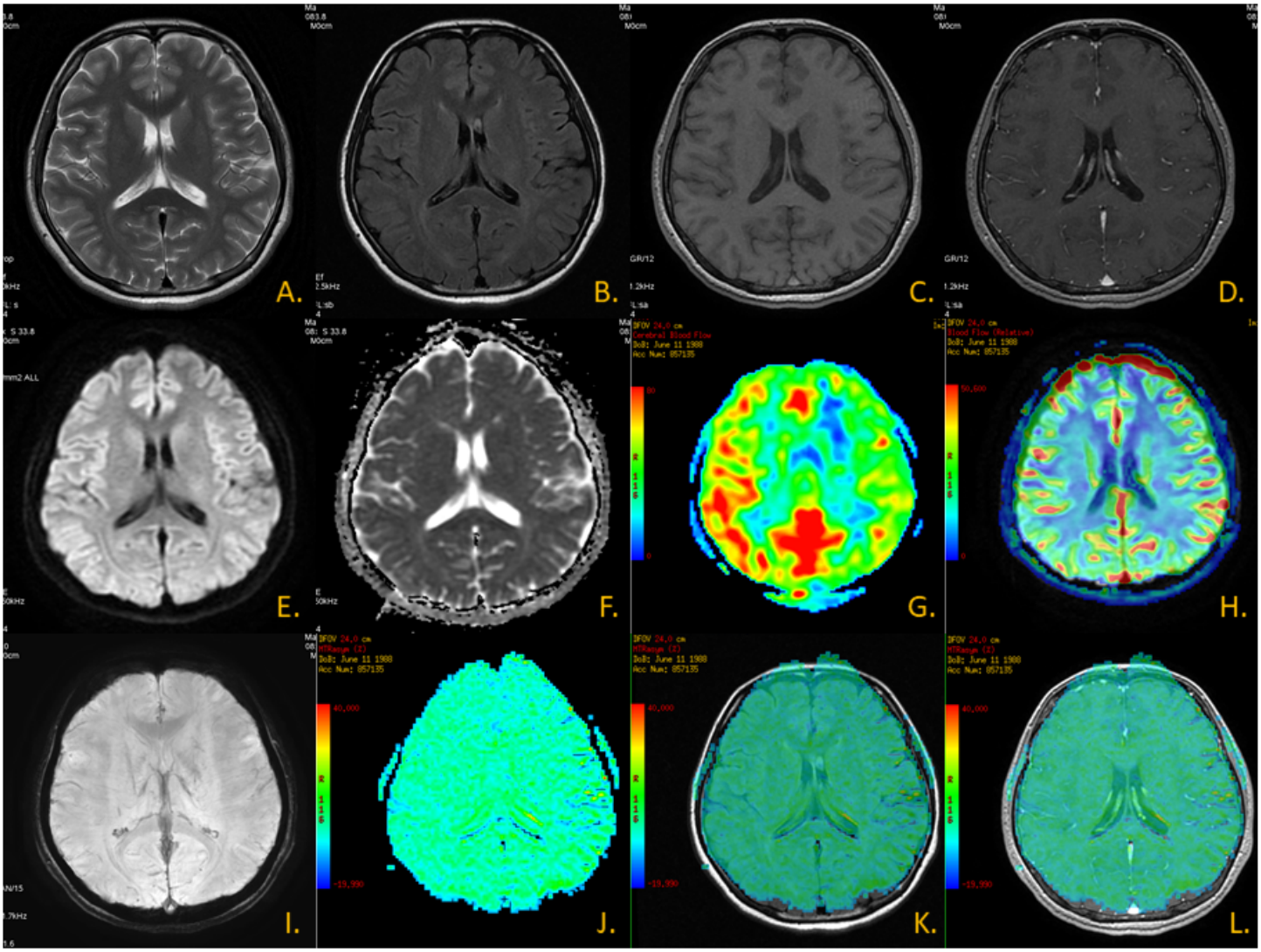

Figure 1

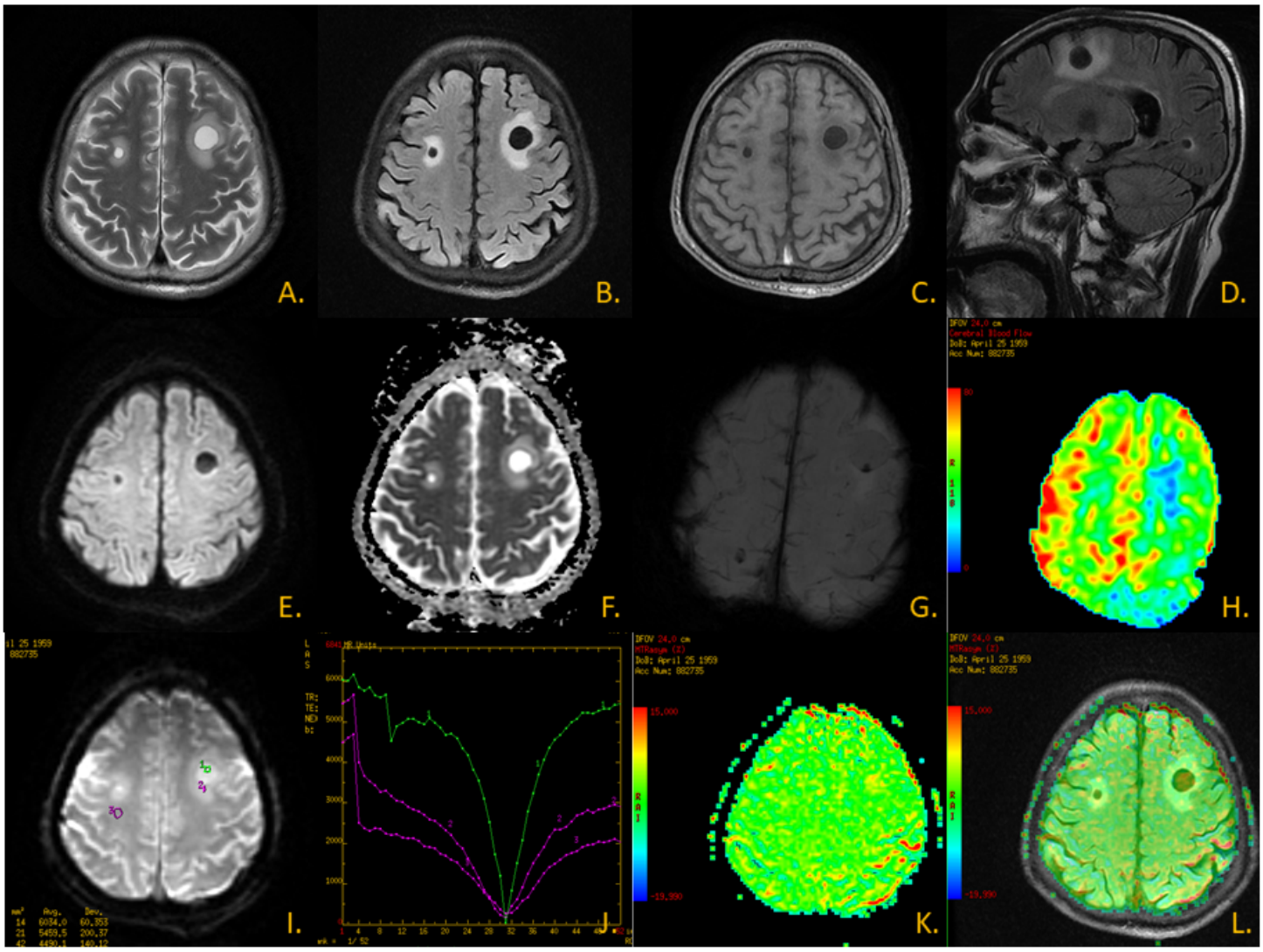

Figure 2

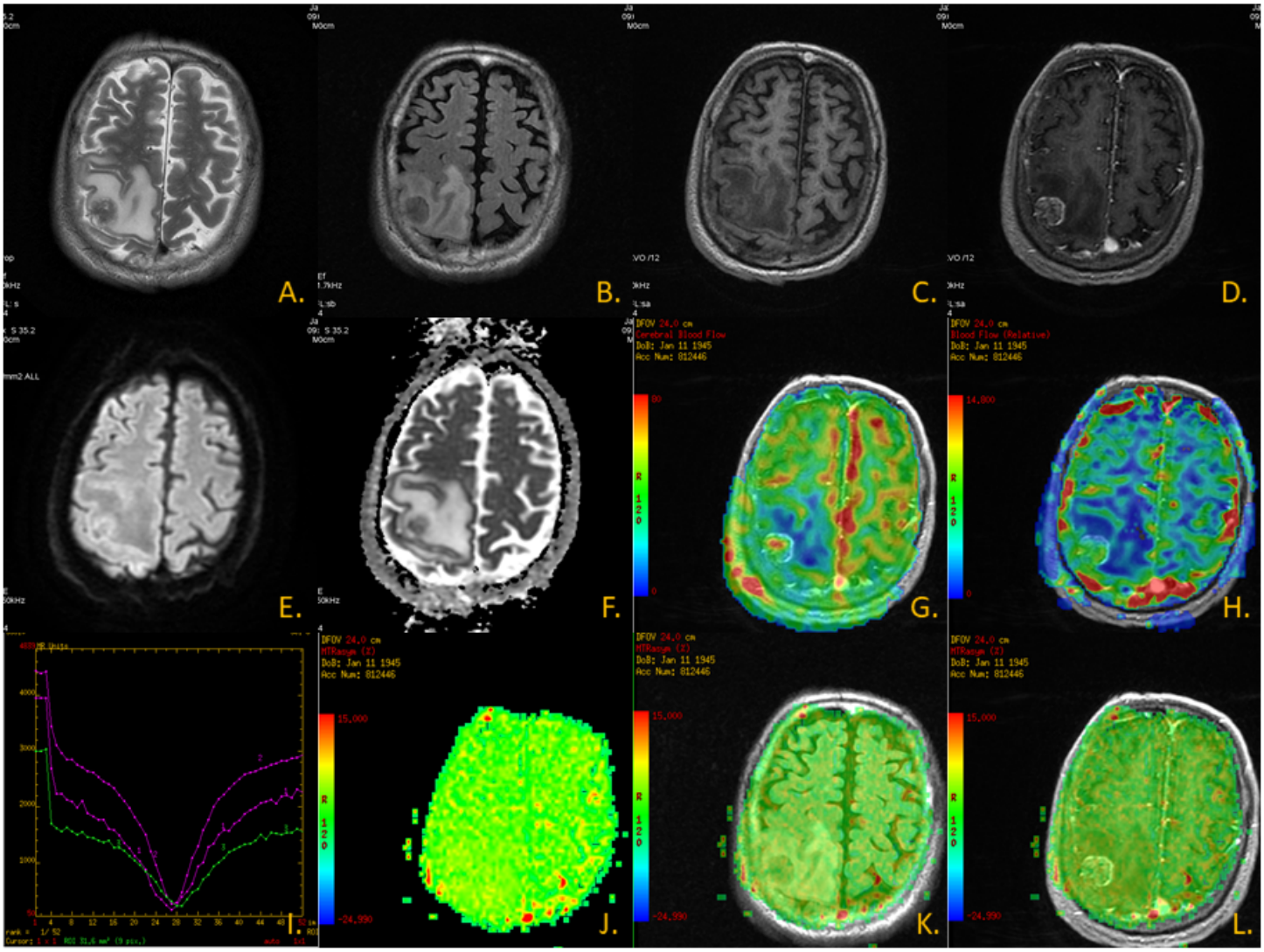

Figure 3

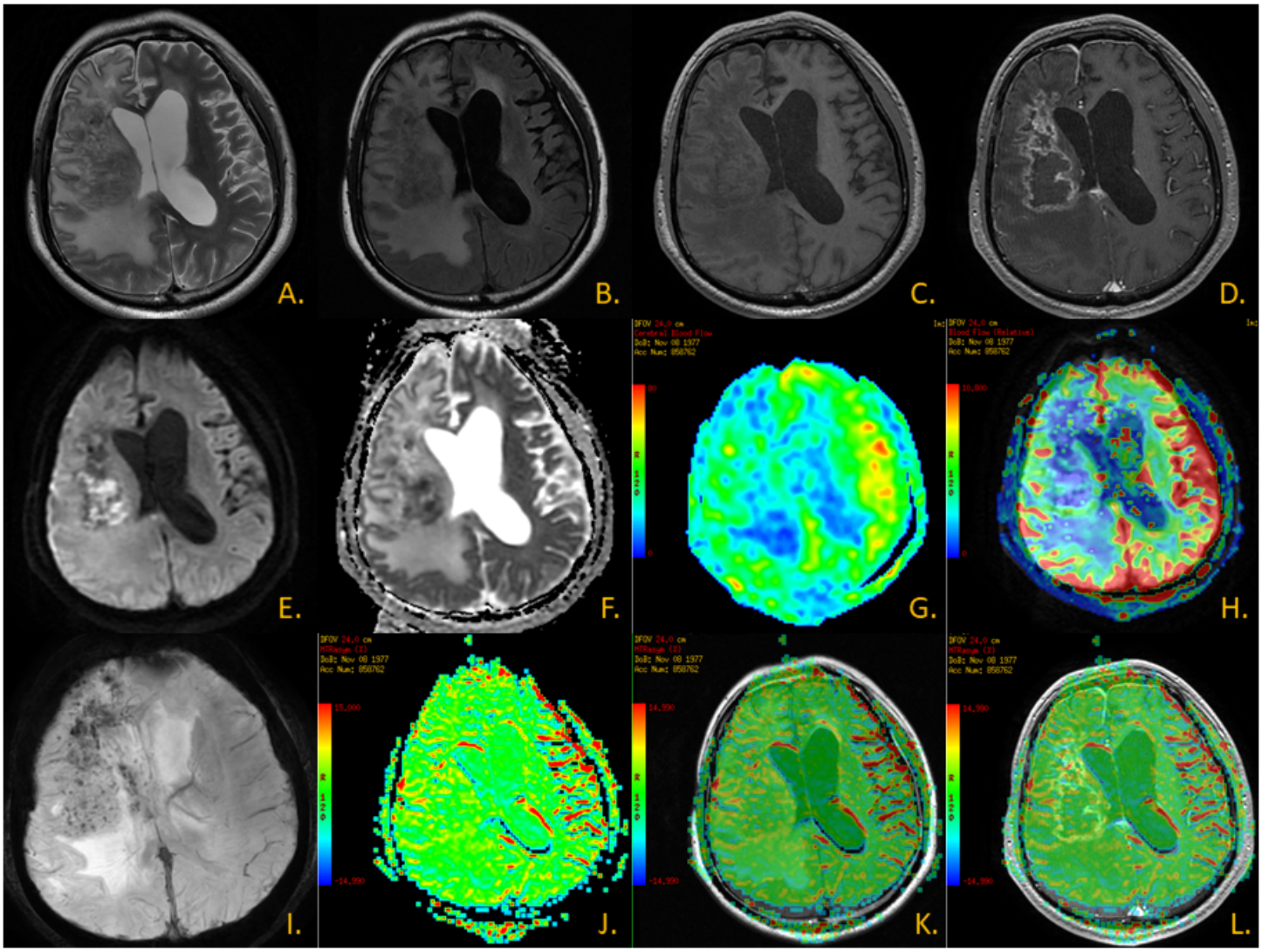

Figure 4

Supplementary Files

This is a list of supplementary files associated with this preprint. Click to download.

- supplement1.jpg